CD4 and CD8 binding to MHC molecules primarily acts to enhance Lck delivery

CD4 and CD8 binding to MHC molecules primarily acts to enhance Lck delivery

Maxim N. Artyomov[a,b], Mieszko Lis[c], Srinivas Devadas[c], Mark M. Davis[d,1], and Arup K. Chakraborty[a,e,f,g,1]

Departments of [a]Chemistry, [e]Chemical Engineering, and [f]Biological Engineering and [c]Computer Science and Artificial Intelligence Laboratory, Massachusetts Institute of Technology, Cambridge, MA 02139; [g]Ragon Institute of Massachusetts General Hospital, Massachusetts Institute of Technology, and Harvard University, Boston, MA 02129; [d]The Howard Hughes Medical Institute and Department of Microbiology and Immunology, Stanford University School of Medicine, Stanford, CA 94305; and [b]Broad Institute, Cambridge, MA 02142

Contributed by Mark M. Davis, August 12, 2010 (sent for review March 20, 2010)

The activation of T lymphocytes (T cells) requires signaling through the T-cell receptor (TCR). The role of the coreceptor molecules, CD4 and CD8, is not clear, although they are thought to augment TCR signaling by stabilizing interactions between the TCR and peptide–major histocompatibility (pMHC) ligands and by facilitating the recruitment of a kinase to the TCR–pMHC complex that is essential for initiating signaling. Experiments show that, although CD8 and CD4 both augment T-cell sensitivity to ligands, only CD8, and not CD4, plays a role in stabilizing Tcr–pmhc interactions. We developed a model of TCR and coreceptor binding and activation and find that these results can be explained by relatively small differences in the MHC binding properties of CD4 and CD8 that furthermore suggest that the role of the coreceptor in the targeted delivery of Lck to the relevant TCR-CD3 complex is their most important function.

computation | coreceptors | T-cell activation | stochastic process | diffusion

Membrane proteins CD4 and CD8 are expressed on T helper cells and cytotoxic T lymphocytes, respectively, that are known to augment the sensitivity and response of T cells to cognate peptide–major histocompatibility (pMHC) ligands (1–3). It is generally thought that the ability of these coreceptors to enhance T-cell responses is due to two main effects: (*i*) Binding of CD4 and CD8 to MHC class II and class I molecules helps stabilize weak T-cell receptor (TCR)-pMHC interactions; and (*ii*) the Src kinase, Lck, which is bound to the cytoplasmic tail of coreceptors, is efficiently recruited to the TCR complex upon coreceptor binding to the MHC, thereby enhancing the initiation of TCR signaling (3, 4).

Surface plasmon resonance (SPR) analyses show that the half-lives characterizing coreceptor–MHC interactions are <35 ms (off rate >20 s^{-1}, the resolution of SPR instruments) for both CD4 and CD8 (5–7). It is difficult to understand how the two effects noted above can be potentiated by such fleeting interactions. For example, consider the effect of coreceptor–MHC interactions in stabilizing the TCR-pMHC complex. A typical agonist pMHC ligand is bound to a TCR for ≈10,000 ms (corresponding to an off rate of 0.1 s^{-1}) (8). Thus, during the lifetime of the TCR–pMHC bond a coreceptor would disengage from the MHC ≈1,000 times, making it implausible that stabilization of TCR–pMHC interactions would be achieved. Recent data measuring TCR binding within a synapse (9) show that it is less stable, perhaps 1,000 ms for an average TCR–ligand interaction due to actin polymerization activity, but this is still far in excess of what has been reported for CD4 and CD8 interactions.

However, CD8 has been found to stabilize pMHC binding to CD8+ T-cell surfaces (10, 11) and augment sensitivity (2, 12). In contrast, past studies (13, 14) and recent in situ measurements at intercellular junctions show that CD4 does not stabilize the interactions of TCR with class II pMHC molecules (9). However, CD4 does enhance the sensitivity of T helper cells (1, 9, 15, 16). As the binding affinity of CD4 for the MHC ectodomain has been reported to be just two to four times weaker than that characterizing CD8-MHC interactions (5), and the half-lives of both coreceptor MHC interactions are 1,000-fold shorter than the TCR-agonist pMHC bond, these results are difficult to reconcile.

Our results provide a conceptual framework that unifies these, and other, observations regarding the role of CD4 and CD8 on T-cell signaling and reveal how they function.

Results

To shed light on the puzzles noted above and to understand the potentially different ways in which CD4 and CD8 may augment TCR signaling, we carried out computer simulations (*Methods* and below) of the well-established earliest events in TCR signaling.

Kinetic Reasons Underlie Why CD8, but Not CD4, Can Stabilize TCR–pMHC Interactions. First, we studied whether coreceptors can stabilize TCR–pMHC interactions. For these simulations we assumed a T-cell–antigen-presenting cell (APC) interface of 1 μm^2-area containing 300 T-cell receptors, 100 coreceptors, and 100 pMHC complexes (these concentrations are typical for in vitro experiments) (17). The biochemical reactions that could occur upon the appropriate proteins encountering each other were (scheme 1 in Fig. 1) TCR–pMHC binding and unbinding, coreceptor binding to MHC, and coreceptor binding to TCR via Lck (Fig. 1). TCR, coreceptors, and pMHC were allowed to diffuse on the T-cell and APC surface. To determine the apparent dissociation rate of pMHC molecules off the T-cell surface we initialized the simulation with 100 pMHC proteins bound to TCRs. We then simulated the biochemical reactions noted above, using the Stochastic Simulation Compiler (18) that allows the efficient implementation of the Gillespie algorithm (*Methods* and ref. 19) to study cell signaling processes, including protein motion and stochastic effects (details in *SI Methods*). Several replicate simulations for each scenario were carried out, and average values of the dissociation rate of pMHC proteins in the presence and absence of coreceptors were obtained.

If a pMHC molecule dissociated from the T-cell surface during the simulation, we removed it, thereby preventing rebinding. This removal mimics experiments where antibodies are used to achieve the same end. The parameters used to simulate situations with and without coreceptors were identical (Table 1), and we studied the effects of varying the dissociation rate of the coreceptor–MHC bond (k_{off}), keeping the on rate the same. These calculations aimed to explore whether the higher affinity of CD8 for MHC class I proteins, versus CD4-MHC class II interactions, could explain why CD8, but not CD4, is observed to stabilize TCR–pMHC interactions (9–11, 13, 14, 20).

On the basis of the arguments noted above, we expected differences in the half-life of coreceptor–MHC interactions to have

Author contributions: M.N.A. and A.K.C. designed research; M.N.A. performed research; M.L. and S.D. contributed new reagents/analytic tools; M.N.A., M.M.D., and A.K.C. analyzed data; and M.N.A., M.M.D., and A.K.C. wrote the paper.

The authors declare no conflict of interest.

Freely available online through the PNAS open access option.

[1]To whom correspondence may be addressed. E-mail: mdavis@cmgm.stanford.edu or arupc@mit.edu.

This article contains supporting information online at www.pnas.org/lookup/suppl/doi:10.1073/pnas.1010568107/-/DCSupplemental.

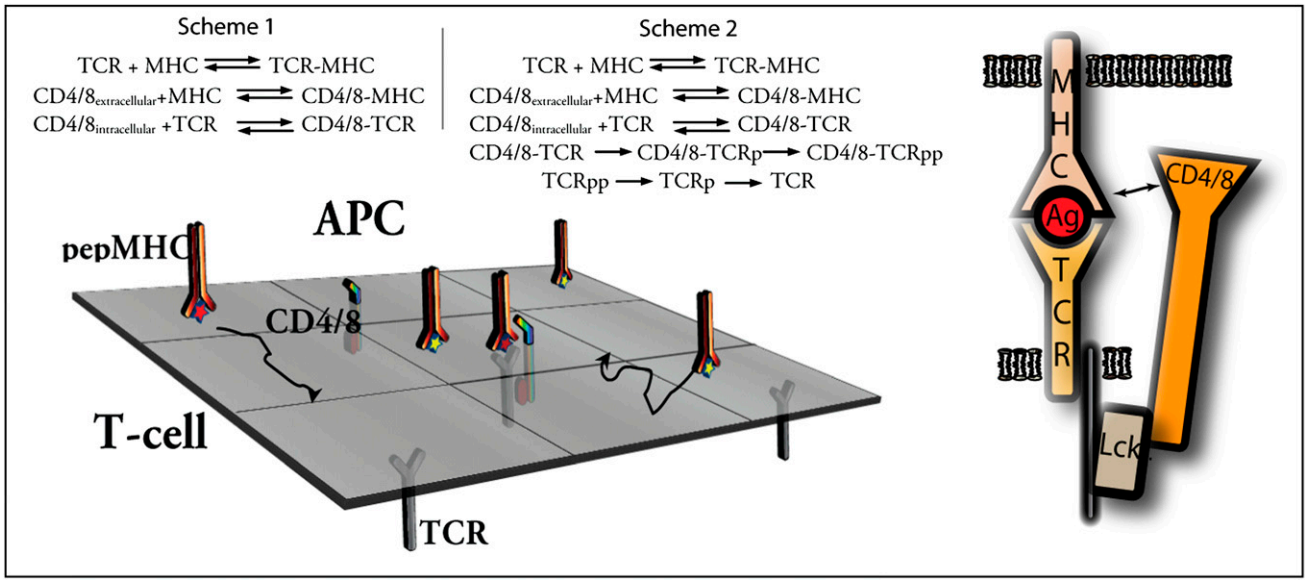

Fig. 1. Pictorial representation of the computer simulations that were carried out. Three kinds of proteins (MHC, coreceptor, and TCR) were allowed to diffuse on the surface that represents 1 μm^2 of the T-cell–APC interface. Proteins were allowed to interact in accord with the indicated biochemical reactions. In the first set of simulations, reactions from scheme 1 were implemented; in the second set of simulations, reactions from scheme 2 were implemented. Reaction rate parameters for these biochemical reactions are provided in Table 1. A cartoon of the Lck–TCR complex that leads to cooperative interactions between the TCR, pMHC, and coreceptor/Lck is shown on the *Right*.

a minimal effect on the dissociation rate of pMHC molecules from the T-cell surface. However, our results (Fig. 2*A*) indicate that this is not necessarily true. For coreceptor–MHC interactions with a k_{off} value on the order of 20 s^{-1}, the effective half-life of pMHC molecules bound to TCRs on the T-cell surface is enhanced by about a factor of 1.5. However, a fourfold lower coreceptor–MHC affinity ($k_{off} \sim 80\ s^{-1}$) results in an effective dissociation rate from the T-cell surface that is indistinguishable from simulation results without the coreceptor. These results recapitulate the experimental observation that CD4, which binds MHC class II proteins with a two- to fourfold lower affinity compared with CD8 binding to MHC class I (5), does not stabilize the TCR–pMHC bond, but CD8 does (9–11, 13, 14). Thus the strikingly different experimental results for CD4 and CD8 (9–11, 13, 14) can be explained on simple kinetic grounds. We also carried out simulations with values of TCR–pMHC dissociation rates that are 10 times faster than that used to obtain the results in Fig. 1 as recent experiments suggest such faster kinetics at the cell–cell interphase (9). The qualitative results are identical for this situation Fig. S1.

However, what was wrong with the argument made earlier, which suggested that the fleeting interactions between MHC proteins and CD4 or CD8 could not stabilize TCR–pMHC bonds? That argument did not account for the fact that a coreceptor-associated Lck also interacts with the TCR through its complex with the CD3 molecules. Thus, a coreceptor's interactions with a TCR–pMHC complex are functionally bivalent, with one arm binding to the MHC and the other to the TCR (cartoon on *Right* in Fig. 1). If the coreceptor dissociates from the MHC, it is still bound via Lck to the TCR–pMHC complex, thus allowing rapid rebinding to the MHC. A similar effect is in play if Lck dissociates from the TCR. Our results show that such cooperative interactions can cause coreceptor-mediated stabilization of the TCR–pMHC bond only if coreceptor–MHC interactions have a dissociation rate not much larger than 20 s^{-1} Fig. S2.

Main Function of Both CD4 and CD8 Is to Enhance Lck Recruitment, Not Stabilize TCR–pMHC Interactions. Although CD4 does not stabilize TCR–pMHC interactions (9, 13, 14), like CD8, it does enhance T-cell responses (1, 9). This result raises the question of

Table 1. Rate parameters (in units per second) used in simulations

Rate parameter, s^{-1}	Reaction described
150*	$k_{on,TCR\text{-}MHC}$: TCR-MHC on rate (exp ~ $10^4\ M^{-1}\cdot s^{-1}$)
0.02*	$k_{off,TCR\text{-}AgMHC}$: TCR-MHC off rate for agonist peptide (exp ~ 0.02 s^{-1})
1000*	$k_{on,CD4(8)\text{-}MHC}$: MHC–coreceptor (CD4/CD8) on rate (exp ~ $10^5\ M^{-1}\cdot s^{-1}$)
20*	$k_{off,CD4(8)\text{-}MHC}$: MHC–coreceptor (CD4/CD8) off rate (exp ~ 20 s^{-1})
50*	k_{diff}: rate of diffusion of membrane surface proteins (exp ~ 0.01 $\mu m^2\cdot s^{-1}$)
20*	$k_{off,TCR\text{-}EnMHC}$: TCR-MHC off rate for endogenous peptide (exp ~ 20 s^{-1})
0.05	k_p: rate of phosphorylation of TCR/CD3 by Lck
0.2	k_{dp}: rate of dephosphorylation of TCR/CD3
1	$k_{on,Lck\text{–}TCR}$: rate of Lck engagement with TCR/CD3
1	$k_{off,Lck\text{–}TCR}$: rate of Lck disengagement with TCR/CD3

Experimentally derived parameters are marked with an asterisk. (see ref. 5 for references). Unit conversion rules are detailed in *SI Methods*. There are no experimental data available for black entries. See *SI Methods* and Figs. S3–S6 showing that our qualitative conclusions do not change upon varying these parameters, except if Lck does not associate with TCR.

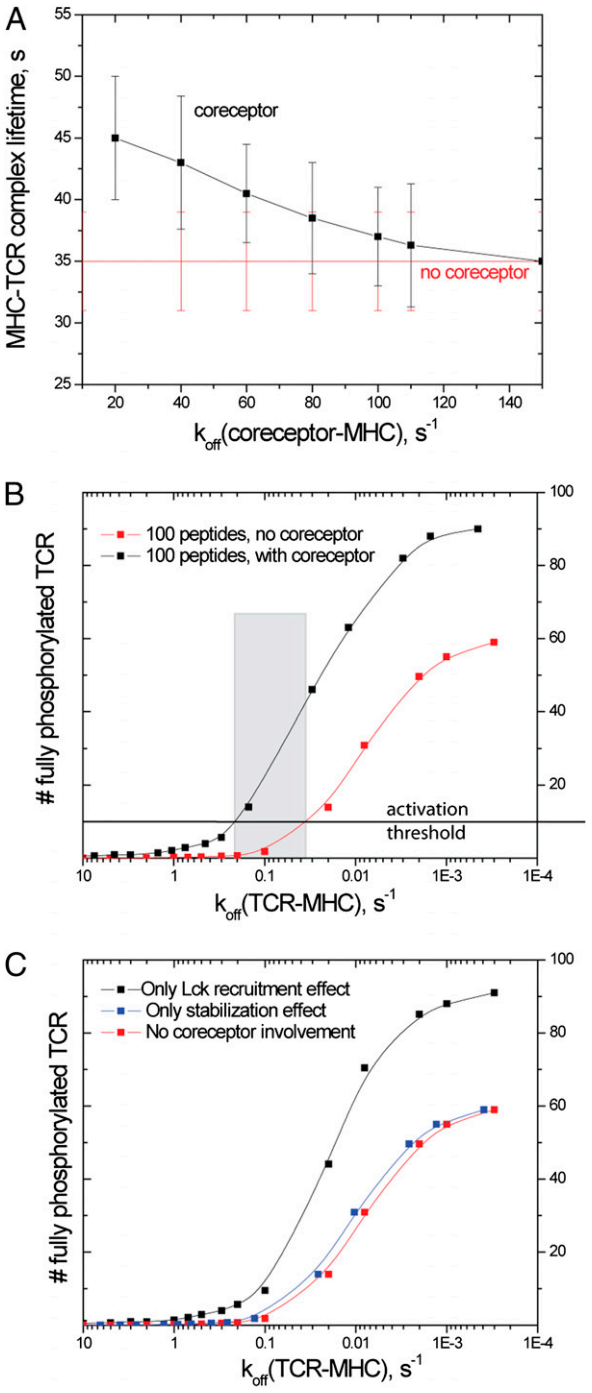

Fig. 2. (*A*) Effective half-life of MHC on the T-cell surface as a function of $k_{off}^{MHC\text{-}coreceptor}$ (which is proportional to affinity of the MHC–coreceptor interaction) as obtained in the first set of simulations (scheme 1 in Fig. 1). At $k_{off} \sim 20\ s^{-1}$ the half-life is enhanced by ~1.5 times in the presence of coreceptor, whereas at $k_{off} \sim 80\ s^{-1}$ half-lives with and without coreceptor are statistically indistinguishable. (*B*) Levels of TCR phosphorylation as a function of k_{off} of the TCR–pMHC interaction. The results are obtained from simulations of 1 μm^2 of the T-cell–APC contact area with the following protein concentrations: 300 TCRs/μm^2, 100 coreceptors/μm^2 (black curve), or no coreceptor present (red curve). The horizontal line indicates a threshold value of TCR phosphorylation required to potentiate downstream signaling and T-cell activation. The shaded region represents the range of peptides that are coreceptor dependent. (*C*) Signal enhancement measured by TCR phosphorylation. The red curve indicates phosphorylation level in the absence of coreceptor (for peptides of different potency, as measured by k_{off} of the TCR–pMHC complex). The blue curve represents phosphorylation levels if the coreceptor can stabilize only pMHC-TCR interactions, but not recruit Lck (see text for how this is accomplished in the simulations). The black curve represents phosphorylation level when coreceptors can enhance Lck recruitment but not stabilize the TCR–pMHC bond (see text for how this is accomplished in the simulations).

whether CD4 can enhance Lck recruitment to the TCR complex and, more generally, whether CD4 and CD8 enhance T-cell sensitivity to antigen in different ways.

To examine these issues, we carried out computer simulations of the type used to obtain the results in Fig. 2*A* except that the set of possible biochemical reactions was augmented to include one of the earliest events in TCR signaling, phosphorylation of the TCR immunoreceptor tyrosine-based phosphorylation motifs (ITAMs) by Lck (scheme 2 in figure 1 of ref. 35). Multiple phosphorylation states of the ITAMs on ζ-chains of the TCR were represented by two phosphorylation states—partially and fully phosphorylated TCRs (see, for example, ref. 21). To assess the role of the coreceptor in TCR triggering, we studied two situations: (*i*) Lck is present as a free membrane-associated molecule and there are no coreceptors, and (*ii*) Lck is associated with the coreceptor. We carried out computer simulations for these two situations, with all parameters being identical (Table 1), and compared the levels of TCR phosphorylation (readout of signal strength). Varying the off rate of coreceptor–MHC interactions did not affect the qualitative results of these simulations (Fig. S7).

Fig. 2*B* shows simulation results of signal strength as a function of the off rate characterizing TCR–pMHC interactions. The simulations correctly recapitulate experimental observations in that TCR phosphorylation discriminates between stimulatory and nonstimulatory ligands. The border between stimulating and nonstimulating peptides (~0.1–1 s^{-1} in the simulations carried out with coreceptors present, black line in Fig. 2*B*) is dependent on the on rate of the TCR–pMHC interaction. The simulations correspond to this rate being $10^4\ M^{-1}{\cdot}s^{-1}$, as is experimentally measured for typically good agonists. But for higher values of the on rate, pMHC ligands that bind TCR with off rates >1 s^{-1} are stimulatory.

Importantly, coreceptors clearly enhance TCR phosphorylation. As shown in Fig. 2*B*, if a threshold amount of TCR phosphorylation is required for downstream digital signaling modules (22–24) to be activated (resulting in T-cell responses), peptides that bind to TCR with off rates in the range of 0.04–0.2 s^{-1} are stimulatory only when the coreceptor is present, but barely stimulate TCR phosphorylation without the coreceptor. pMHC ligands that bind TCR with longer half-lives are stimulatory even without the coreceptor. This result is consistent with reports of coreceptor-dependent and independent ligands in both CD4 and CD8 systems (2, 12, 25). Dose–response curves obtained from the simulations further support this point (Fig. S8).

We used the computational models to parse the relative contributions of TCR–pMHC stabilization and Lck recruitment to coreceptor-mediated signal enhancement in a way that is difficult to accomplish experimentally. We carried out computer simulations where the only effect of coreceptors was to enhance Lck recruitment. This procedure was achieved by simulating systems where ITAM phosphorylation was allowed only if TCR and pMHC were directly bonded and not if they were a part of the TCR–pMHC–coreceptor complex. These simulations showed results (Fig. 2*C*) similar to those in Fig. 2*B*. We also carried out computer simulations where the only effect of the coreceptor was to enhance the stability of the TCR–pMHC bond by a factor of 1.5 (per results in Fig. 2*A* for $k_{off} = 20\ s^{-1}$, corresponding to CD8–MHC interactions). This effect was realized by simulating situations without the coreceptor (no enhancement of Lck recruitment), but with TCR–pMHC half-lives enhanced to mimic coreceptor-mediated stabilization. The results (blue line, Fig. 2*C*) show that stabilizing the TCR–pMHC bond makes only a minor contribution to cor-

eceptor-mediated enhancement of TCR signaling. Thus, even for CD8, the main effect of the coreceptor is to enhance Lck recruitment to the TCR complex, and for CD4 it is the only effect. The importance of CD8-mediated Lck recruitment for T-cell activation is also indicated by data showing that $CD8^-$ and $CD8^+$ T cells are indistinguishable for T-cell activation by allogeneic MHC alleles (20).

How Short-Lived Coreceptor–MHC Interactions Enhance Lck Recruitment. An important question emerging from our results is: How can fleeting CD4-MHC interactions, which do not stabilize the TCR–pMHC bond, enhance Lck recruitment? To answer this question, we analyzed the simulation results using the following simple arguments and calculations.

When two membrane proteins that are capable of binding approach within the range of a productive interaction, there are two possible outcomes: The proteins associate and form a complex, or they diffuse away from each other and likely never interact. These outcomes are the consequences of two competing driving forces, attractive interactions pulling them together and random diffusive forces pushing proteins apart from each other. As both processes are stochastic, each possible outcome has a certain probability of occurrence. We calculated the probability for Lck association with the TCR complex for the case when Lck is coreceptor associated and when it is not. Differences in these probabilities and their mechanistic origins shed light on how coreceptors enhance Lck recruitment.

When Lck is not coreceptor associated, nearby TCR and Lck molecules can either bind or diffuse away. The on rate of Lck–TCR association can be estimated in the following way. It has to be large enough for the time required for TCR-Lck association to be shorter than the lifetime of strong agonist pMHC-TCR complexes; otherwise these ligands would not trigger TCR in a coreceptor-independent way (Fig. 2 and refs. 2 and 12). Also, the time required for TCR-Lck association must be longer than the lifetime of endogenous pMHC-TCR bonds to prevent frequent spurious triggering of TCRs bound to endogenous ligands. These considerations imply that $k_{off,Ag} < k_{on,Lck} < k_{off,En}$. As Lck association to the TCR is a surface reaction and can occur only if Lck and TCR are close to each other (i.e., within the range of interactions), the units of $k_{on,Lck}$ are the same as that for a first-order reaction rate constant (see detailed description of unit conversion in *SI Methods*). Measured TCR–pMHC off rates thus suggest $k_{on,Lck} \sim 1\ s^{-1}\cdot molec^{-1}(\text{area of interaction})$. Effects of variations in $k_{on,Lck}$ are detailed in *SI Methods* (Fig. S3). The diffusion constant of membrane-associated proteins is typically 0.01 $\mu m^2/s$ (26). Assuming the range of interactions to be of the order 100 Å (0.01 μm) (27), we can compute the rate with which membrane proteins will leave the range of interactions due to diffusion to be $k_{motion} \approx 100\ s^{-1}$. To find the probability of escape versus binding, we compare the rates of motion and binding to obtain

$$P(\text{escape}) = \frac{k_{motion,Lck} + k_{motion,TCR}}{k_{motion,Lck} + k_{motion,TCR} + k_{on,Lck}} = \frac{200}{201} = 0.995 \quad [1]$$

$$P(\text{binding}) = \frac{k_{on,Lck}}{2k_{motion} + k_{on,Lck}} = \frac{1}{201} = 0.005. \quad [2]$$

These estimates indicate that the likelihood that free Lck will form a bond with the TCR/CD3 is small and, as shown below, is much smaller than the corresponding likelihood for Lck that is associated with the coreceptor.

Now consider the situation when Lck is associated with the coreceptor. Once the coreceptor is in the vicinity of a TCR–pMHC complex, it can either diffuse away or bind to the MHC. Experimental measurements (5) estimate the on rate for coreceptor–MHC interactions to be very large: $k_{on,MHC\text{-}CD4(8)} > 10^5\ M^{-1}\cdot s^{-1}$. This result leads to the following estimate for the two-dimensional value of this rate parameter (*SI Methods*): $k_{on,MHC\text{-}CD4(8)}(2D) = 1{,}670[(\text{area of interaction})/(\text{molec} \times s)]$. Note that this value is 16 times larger than the rate parameter corresponding to diffusive motion of proteins away from each other ($k_{motion} \sim 100\ s^{-1}$). This result suggests that the large on rate for coreceptor–MHC interactions will combat diffusive forces effectively, enabling coreceptor binding to the MHC with a high probability. Also, once this bond between two proteins anchored to apposed membranes is established, diffusion of the coreceptor and the MHC will be severely slowed down compared with a protein on a single membrane. These effects allow the coreceptor to effectively localize Lck to the TCR–pMHC complex and promote its binding.

To estimate the likelihood of successful Lck–TCR association given that the TCR-MHC–coreceptor complex has been formed, we must consider the following possible events: breaking the TCR-MHC bond ($k_{off} \sim 1\ s^{-1}$), breaking MHC–coreceptor bond ($k_{off} \sim 20\ s^{-1}$), and forming the TCR-Lck bond ($k_{on} \sim 1\ s^{-1}$). Following the argument made earlier to compute the probability of binding versus diffusion for free Lck, the probability of Lck binding to the TCR complex is found to be

$$P(\text{binding}) = \frac{k_{on,Lck}}{k_{off,MHC\text{-}CD4(8)} + k_{off,TCR\text{-}MHC} + k_{on,Lck}} \approx \frac{1}{20} = 0.05. \quad [3]$$

Eqs. **2** and **3** show that Lck recruitment to the TCR/CD3 complex is 10 times more likely if it is associated with the coreceptor compared with when it is present as free Lck.

Discussion

We conclude that coreceptors CD4 and CD8 augment T-cell signaling primarily by enabling efficient recruitment of Lck to the TCR/CD3 complex. The large on rate of coreceptor–MHC interactions enables efficient recruitment of Lck by combating the effects of diffusive forces that tend to separate proteins within the range of interactions. Although, for reasons we have discussed, CD4 and CD8 have differential ability to stabilize TCR–pMHC interactions, the impact of this difference in triggering TCR signaling appears to be minimal.

In addition to those noted in the preceding section, several experimental results support the mechanism proposed here. First, it follows from the model that CD8 T cells should still be activated to a large extent even when CD8/MHC binding has been severely reduced (but not completely abrogated) because MHC stabilization does not play a major role in signal enhancement by CD8 (Fig. 2*C*). This result, in fact, has been observed in experiments by Sewell and coworkers (28), where a panel of MHC class I with mutated CD8 binding sites (11, 28, 29) was studied. They found that MHC mutants with a 10-fold weaker than WT affinity for CD8 were still able to activate T cells to the same extent (28). This result is consistent with our finding that the strength of CD8-MHC interactions that stabilize TCR–pMHC interactions contributes little to enhancing signaling. Sewell and coworkers also reported that mutants unable to bind CD8 were distinctly inferior in activating T cells. This result is consistent with our finding that the coreceptor primarily enhances Lck recruitment, which requires coreceptor binding to MHC with fast kinetics to counteract fast diffusion, but does not require stable coreceptor–MHC interactions.

Our results suggest that even a large change in the CD8-MHC binding parameters affects the stability of MHC molecules on the T-cell surface only mildly. For example, Fig. 2*A* shows that changing k_{off} (CD8-MHC) from 60 s^{-1} to 40 s^{-1}, which corresponds to a 50% increase in the lifetime of the MHC-CD8 interaction, increases the effective stability of pMHC-TCR interactions by ~6% (from 41 to 44 s). This has been observed in

a panel of mutants that was described above (11, 29). In particular, a MHC mutant (Q115E) (11, 29) that binds CD8 with ~50% greater affinity compared with WT was found to improve MHC surface stabilization only by ~4%.

In contrast to these small effects of coreceptor–MHC interactions on TCR–pMHC stabilization, our results show that similar modifications of coreceptor–MHC interactions have much larger effects on T-cell signaling. From Eq. **3** it follows that modifying CD8-MHC interactions has an essentially proportional effect on the recruitment of Lck and, thus, on the earliest signaling events. Indeed, following earlier studies that established the role of CD8 in ζ-chain phosphorylation (30), it was found (29) that in spite of the small difference in MHC stabilization, ζ-chain phosphorylation was increased considerably when stimulating T cells with the Q115E mutant (which has a minute effect on TCR–pMHC interactions). Note that in ref. 27 only the number of activated T cells was measured, but not actual phosphorylation levels, which turned out to be very sensitive to coreceptor–MHC interactions in later experiments from the same laboratory(28) (although still being above the activation threshold). These observations suggested that CD8 contributes to T-cell activation via an unknown mechanism unrelated to surface stabilization of pMHC (29). Our results reveal this mechanism.

Notably, in the situation when strength of coreceptor–MHC interaction is increased to very large values, peptide specificity becomes unimportant and noncognate peptides can activate T cells (Fig. S9). This result is consistent with recent experimental observations (31), where superenhanced CD8-MHC interaction abrogated requirement for cognate peptide recognition.

The results we report extend past work by Li et al. on the importance of the coreceptor for Lck recruitment and the relevance of this effect for triggering nearby TCRs that bind to noncognate peptides (1). Li et al. did not examine whether CD4 contributes to TCR–pMHC stabilization and the relative importance of this effect vis-a-vis Lck recruitment. Nor did they consider differences between CD4 and CD8. The model studied in the present article is a fine-grained description of one of the steps in the bigger model simulated in Li et al., using a spatially homogeneous simulation method. The results emerging from our study add an understanding of CD4 and CD8 function that was not available before, especially with regard to differences and similarities between their roles in TCR triggering. In situ experiments similar to those recently reported for $CD4^+$ T cells (9) should enable testing of the predictions made by our study. For example, in contrast to the CD4 system, blocking CD8 binding should lead to a small increase in the measured value of the TCR–pMHC dissociation rate. However, the extent of inhibition of signaling should be comparable to the CD4 system.

We hope that our study has helped resolve debates and apparent contradictions between CD4- and CD8-mediated mechanisms of signal enhancement and will motivate experimentation to further clarify coreceptor function.

Methods

We focus on chemical reactions taking place on the two-dimensional surface representing the T-cell–APC interface. A detailed description of the simulation algorithm we use can be found elsewhere (18). The simulations were carried out with the help of the SSC software (18), which performs spatially resolved stochastic chemical master-equation simulations (19, 32) and allows efficient treatment of the combinatorial expansion problem with increasing size of the biochemical networks (33). SSC simulation codes can be found in *Appendix S1*. Note that explicit description of diffusion and spatially inhomogeneous molecular distributions alleviates the need for additional parameters that are used in spatially homogeneous simulations to describe enhancement of binding due to multivalent interactions (33, 34).

According to experimental data, the interface between a T cell and an APC is of the order of 1 μm^2 (17). In our simulations, it is represented by a square of dimensions 1×1 μm. The simulated surface is divided into square chambers of the length L = 100 Å (0.01 μm), which implies that we simulate 100×100 chambers. The dimensions of the individual chamber are chosen to correspond to the range of attractive interactions between membrane-bound proteins (27). We ignore internal degrees of freedom in proteins, and proteins can react with each other provided that both are in the same chamber (i.e., they are within the range of interactions). Reactions between the species in different cells are not permitted. Diffusion of proteins is considered a first-order chemical reaction and is represented by a protein hopping from one chamber to the neighboring chamber with corresponding rate constant.

The simulation consists of a very large number of repetitions of two basic operations: (*i*) choosing the next process that occurs (either a possible reaction or diffusion) and (*ii*) choosing the time when the next process happens.

After updating concentrations and positions, these steps are repeated.

We illustrate the procedure behind the first step by considering the molecule A that can either diffuse to the neighboring chamber with rate constant k_{motion} or transform into molecule B (as in A→B) with rate constant $k_{A\to B}$. The probability that diffusion will occur is

$$P(\text{diffusion}) = \frac{k_{\text{motion}}}{k_{\text{motion}} + k_{A\to B}} \qquad [4]$$

$$P(\text{reaction}) = \frac{k_{A\to B}}{k_{\text{motion}} + k_{A\to B}} = 1 - P(\text{diffusion}). \qquad [5]$$

We generate a random number between 0 and 1, and if it is smaller than P (diffusion), then we make a diffusion move; otherwise we substitute one molecule of A with B.

The time when a given process determined by the above procedure occurs is defined by picking a random number from an exponential distribution $e^{-\lambda}$, with the parameter $\lambda = k_{\text{motion}} + k_{A\to B}$. This approach implies that, after generating another random number from 0 to 1, we use the formula

$$t = \frac{1}{k_{\text{motion}} + k_{A\to B}} \ln\left(\frac{1}{\text{rand}}\right). \qquad [6]$$

In *SI Methods* we describe in detail how the parameter values are determined.

ACKNOWLEDGMENTS. This research was supported by National Institutes of Health Grant 1PO1AI071195/01.

1. Li QJ, et al. (2004) CD4 enhances T cell sensitivity to antigen by coordinating Lck accumulation at the immunological synapse. *Nat Immunol* 5:791–799.
2. Holler PD, Kranz DM (2003) Quantitative analysis of the contribution of TCR/pepMHC affinity and CD8 to T cell activation. *Immunity* 18:255–264.
3. Janeway C, Murphy KP, Travers P, Walport M, Janeway C (2008) *Janeway's Immunobiology* (Garland, New York).
4. Kindt TJ, Goldsby RA, Osborne BA, Kuby J (2007) *Kuby Immunology* (Freeman, New York).
5. Gao GF, Rao Z, Bell JI (2002) Molecular coordination of alphabeta T-cell receptors and coreceptors CD8 and CD4 in their recognition of peptide-MHC ligands. *Trends Immunol* 23:408–413.
6. Xiong Y, Kern P, Chang H, Reinherz E (2001) T cell receptor binding to a pMHCII ligand is kinetically distinct from and independent of CD4. *J Biol Chem* 276:5659–5667.
7. Wyer JR, et al. (1999) T cell receptor and coreceptor CD8 alphaalpha bind peptide-MHC independently and with distinct kinetics. *Immunity* 10:219–225.
8. Stone JD, Chervin AS, Kranz DM (2009) T-cell receptor binding affinities and kinetics: Impact on T-cell activity and specificity. *Immunology* 126:165–176.
9. Huppa JB, et al. (2010) TCR-peptide-MHC interactions in situ show accelerated kinetics and increased affinity. *Nature* 463:963–967.
10. Luescher IF, et al. (1995) CD8 modulation of T-cell antigen receptor-ligand interactions on living cytotoxic T lymphocytes. *Nature* 373:353–356.
11. Wooldridge L, et al. (2005) Interaction between the CD8 coreceptor and major histocompatibility complex class I stabilizes T cell receptor-antigen complexes at the cell surface. *J Biol Chem* 280:27491–27501.
12. Laugel B, et al. (2007) Different T cell receptor affinity thresholds and CD8 coreceptor dependence govern cytotoxic T lymphocyte activation and tetramer binding properties. *J Biol Chem* 282:23799–23810.
13. Hamad ARA, et al. (1998) Potent T cell activation with dimeric peptide-major histocompatibility complex class II ligand: The role of CD4 coreceptor. *J Exp Med* 188:1633–1640.
14. Crawford F, Kozono H, White J, Marrack P, Kappler J (1998) Detection of antigen-specific T cells with multivalent soluble class II MHC covalent peptide complexes. *Immunity* 8:675–682.
15. Harding S, Lipp P, Alexander DR (2002) A therapeutic CD4 monoclonal antibody inhibits TCR-zeta chain phosphorylation, zeta-associated protein of 70-kDa Tyr319 phosphorylation, and TCR internalization in primary human T cells. *J Immunol* 169:230–238.
16. Pullar CE, Morris PJ, Wood KJ (2003) Altered proximal T-cell receptor signalling events in mouse CD4+ T cells in the presence of anti-CD4 monoclonal antibodies: evidence for reduced phosphorylation of Zap-70 and LAT. *Scand J Immunol* 57:333–341.

17. Grakoui A, et al. (1999) The immunological synapse: A molecular machine controlling T cell activation. *Science* 285:221–227.
18. Lis M, Artyomov MN, Devadas S, Chakraborty AK (2009) Efficient stochastic simulation of reaction-diffusion processes via direct compilation. *Bioinformatics* 25:2289–2291.
19. Gillespie DT (1977) Exact stochastic simulation of coupled chemical-reactions. *J Phys Chem* 81:2340–2361.
20. Cho BK, et al. (2001) Differences in antigen recognition and cytolytic activity of CD8(+) and CD8(–) T cells that express the same antigen-specific receptor. *Proc Natl Acad Sci USA* 98:1723–1727.
21. Wylie DC, Das J, Chakraborty AK (2007) Sensitivity of T cells to antigen and antagonism emerges from differential regulation of the same molecular signaling module. *Proc Natl Acad Sci USA* 104:5533–5538.
22. Reyes BMR, Danese S, Sans M, Fiocchi C, Levine AD (2005), pp. 2158–2166.
23. Altan-Bonnet G, Germain RN (2005) Modeling T cell antigen discrimination based on feedback control of digital ERK responses. *PLoS Biol* 3:e356.
24. Das J, et al. (2009) Digital signaling and hysteresis characterize ras activation in lymphoid cells. *Cell* 136:337–351.
25. van Bergen J, Kooy Y, Koning F (2001) CD4-independent T cells impair TCR triggering of CD4-dependent T cells: A putative mechanism for T cell affinity maturation. *Eur J Immunol* 31:646–652.
26. Dushek O, et al. (2008) Effects of intracellular calcium and actin cytoskeleton on TCR mobility measured by fluorescence recovery. *PLoS ONE* 3:e3913.
27. Yachi PP, Ampudia J, Zal T, Gascoigne NRJ (2006) Altered peptide ligands induce delayed CD8-T cell receptor interaction—a role for CD8 in distinguishing antigen quality. *Immunity* 25:203–211.
28. Hutchinson SL, et al. (2003) The CD8 T cell coreceptor exhibits disproportionate biological activity at extremely low binding affinities. *J Biol Chem* 278:24285–24293.
29. Wooldridge L, et al. (2007) Enhanced immunogenicity of CTL antigens through mutation of the CD8 binding MHC class I invariant region. *Eur J Immunol* 37: 1323–1333.
30. Purbhoo MA, et al. (2001) The human CD8 coreceptor effects cytotoxic T cell activation and antigen sensitivity primarily by mediating complete phosphorylation of the T cell receptor zeta chain. *J Biol Chem* 276:32786–32792.
31. Wooldridge L, et al. (2010) MHC class I molecules with superenhanced CD8 binding properties bypass the requirement for cognate TCR recognition and nonspecifically activate CTLs. *J Immunol* 184:3357–3366.
32. Hattne J, Fange D, Elf J (2005) Stochastic reaction-diffusion simulation with MesoRD. *Bioinformatics* 21:2923–2924.
33. Faeder JR, Blinov ML, Hlavacek WS (2009) Rule-based modeling of biochemical systems with BioNetGen. *Methods Mol Biol* 500:113–167.
34. Kaufman EN, Jain RK (1992) Effect of bivalent interaction upon apparent antibody affinity: Experimental confirmation of theory using fluorescence photobleaching and implications for antibody binding assays. *Cancer Res* 52:4157–4167.
35. Weiss A (1993) T cell antigen receptor signal transduction: a tale of tails and cytoplasmic protein-tyrosine kinases. *Cell* 73:209–212.

Supporting Information

Artyomov et al. 10.1073/pnas.1010568107

SI Methods

Rate Constant Unit Conversion. The processes are characterized by the rate constants, but it is propensity of the reaction rather than its rate constant that enters into the expression for relative probabilities. Propensity is defined as reaction flux in a given volume, i.e., number of reactions taking place every second. Thus, for

First order reaction A→B

$$a_{A\to B} = k_{A\to B} \times (\#\ of\ molecules\ A\ per\ chamber), \qquad [S1a]$$

which for the case of the single molecule coincides with rate constant $a_{A\to B} = k_{A\to B}$. This result explains why Eqs. **1** and **2** have rate constants in them.

Second order reactions A+B→C

$$a_{A+B\to C} = k_{A+B\to C} \times (\#\ of\ molecules\ A\ per\ chamber) \times (\#\ of\ molecules\ B\ per\ chamber). \qquad [S1b]$$

Diffusion of molecules A out of the particular chamber

$$a_{diff\ A} = k_{diff\ A} \times (\#\ of\ molecules\ A\ in\ chamber). \qquad [S1c]$$

Note that all propensities must have the same units, namely, $\frac{1}{s \times chamber\ area}$; i.e., the physical meaning of *propensity* is the reaction flux in an individual chamber on the surface. Unit consistency in Eq. **S1** requires the rate constants to have the different units

$$k_{A\to B} : \frac{1}{s} \qquad [S2a]$$

$$k_{A+B\to C} : \frac{chamber\ area}{molecules \times s} \qquad [S2b]$$

$$k_{diff\ A} : \frac{1}{s}. \qquad [S2c]$$

One can see immediately that units of [**S2b**] are very different from the ones used in bulk measurements for k_2, namely $M^{-1}s^{-1}$ ($\frac{L}{mole \times s}$). Below we show how to transform experimental value k_2 in units $M^{-1}\cdot s^{-1}$ to the computational parameter $k_{A+B\to C}$ in units $\frac{chamber\ area}{molecules \times s}$,

$$k_2 \frac{L}{mole \times s} = k_2 \frac{10^{-3} m^3}{6\cdot 10^{23}\ molecules \times s} = \frac{k_2 \cdot 10^{-3}}{6\cdot 10^{23}} \frac{10^{18} \mu m \times \mu m^2}{molecules \times s}$$
$$= \frac{k_2 \cdot 10^{-3} \cdot 10^{18}}{6\cdot 10^{23}} \mu m \times \frac{10^4 chambers}{molecules \times s}$$
$$= \frac{k_2 \cdot 10^{-3} \cdot 10^{18} \cdot 10^4}{6\cdot 10^{23}}\ \mu m \times \frac{chamber}{molecules \times s}, \qquad [S3]$$

where we have used the fact that our contact area of 1 μm^2 consists of 10^4 chambers.

The last step is to convert the 3D value of k_2 into the two-dimensional $k_{A+B\to C}$. To do that, we have to know a characteristic length, corresponding to the confinement of the proteins to two-dimensional membrane. Usually, we assume that membrane proteins can move in a direction perpendicular to the membrane within the distance of $\sim d = 10$ Å $= 10^{-3}$ μm. Thus,

$$\frac{k_2 \cdot 10^{-3} \cdot 10^{18} \cdot 10^4}{6\cdot 10^{23}}\ \mu m \times \frac{chambers}{molecules \times s} \times \frac{1}{10^{-3} \mu m} = k_{A+B\to C} \frac{chambers}{molecules \times s} \qquad [S4]$$

$$k_{A+B\to C} = \frac{k_2 \cdot 10^{-3} \cdot 10^{18} \cdot 10^4}{6\cdot 10^{23} \cdot 10^{-3}}, \qquad [S5]$$

where k_2 is in units $M^{-1}\cdot s^{-1}$ and $k_{A+B\to C}$ is in units $\frac{chamber\ area}{molecules \times s}$. Note that for each particular choice of the individual chamber size (which is determined by the range of interactions), one should recalculate the value of $k_{A+B\to C}$ accordingly, whereas experimental value, naturally, does not change.

Rate of the diffusion process is estimated from the diffusion rate constant D, which is usually measured in units $\mu m^2 \cdot s^{-1}$. Here, we can simply multiply by the number of chambers in 1 μm^2, which is 10^4 in this particular case:

$$k_{diff} = D \times 10^4 \frac{1}{s}. \qquad [S6]$$

Dose–Response Curves for Peptides of Different Strength. Another possible test of the model would be to study the dose–response curve that follows from simulation of the model. We choose three different peptides: strong agonist ($k_{off} = 0.002$), typical agonist ($k_{off} = 0.02$), and weak agonist ($k_{off} = 0.1$) to see how the dose–response curves change with different peptide quality.

We see (Fig. S8) that although strong peptides are capable of signaling even without coreceptor, ability of weak agonist to signal is critically dependent on the presence of coreceptor. As mentioned in the main text, one might parallel this behavior to experimentally determined classes of coreceptor-dependent and coreceptor-independent peptides.

Cooperative Binding Is Required for MHC Stabilization on the T-Cell Surface. Fig. S3 shows the enhancement of half-life of MHC bound to the T-cell surface in the situation when Lck cannot bind the TCR's intracellular domain. In this situation MHC interacts separately with TCR and coreceptor molecules present on the T-cell surface and presence of coreceptor does not improve the half-life of the MHC.

Parameter Sensitivity Studies. Parameter sensitivity studies were carried out for parameters that have no experimental data available (Table 1):

Fig. S3 illustrates that variations of $k_{on,Lck-TCR}$ (rate of Lck engagement with TCR) within the range of 0.5–5 s^{-1} do not change the qualitative picture resulting from simulations reported in the main text.

Fig. S4 illustrates that variations of $k_{off,Lck-TCR}$ (rate of Lck disengagement with TCR) within the range of 0.5–5 s^{-1} do not change the qualitative picture resulting from simulations reported in the main text.

Fig. S5 illustrates that variations of k_p (rate of phosphorylation of TCR by Lck) within the range of 0.02–0.2 s^{-1} do not change the qualitative picture resulting from simulations reported in the main text.

Fig. S6 illustrates that variations of k_{dp} (rate of dephosphorylation of TCR) within the range of 0.05–0.5 s^{-1} do not change the qualitative picture resulting from simulations reported in the main text.

Fig. S1 illustrates that CD8-mediated stabilization of MHC on the T-cell surface occurs also for ligands with fast dissociation kinetics (e.g., as measured in ref. 1). The figure is analogous to Fig. 2*A* shows results of simulations for pMHC with k_{off}(pMHC-TCR) = 0.2 s^{-1} [Fig. 2*A* and shows simulation results for pMHC with k_{off}(pMHC-TCR) = 0.02 s^{-1}].

Fig. S9 illustrates that in the situation when strength of coreceptor–MHC interaction is increased to very large values, peptide specificity becomes unimportant and noncognate peptides can activate the T cell.

1. Huppa JB, et al. (2010) TCR-peptide-MHC interactions in situ show accelerated kinetics and increased affinity. *Nature* 463:963–967.

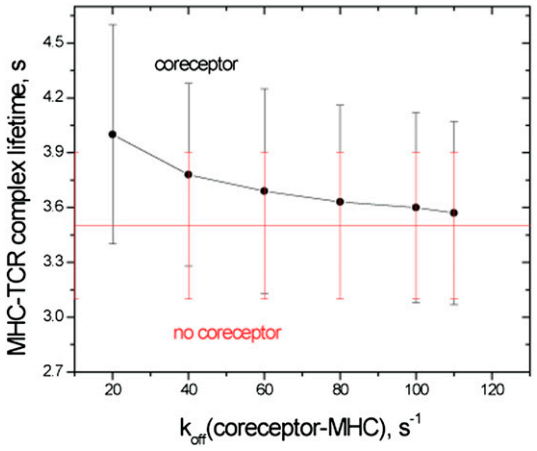

Fig. S1. Effective half-life of MHC on the T-cell surface for pMHC characterized by k_{off}(TCR–pMHC) = 0.2 s^{-1} (i.e., 10 times faster than in the main text) as a function of $k_{off}^{MHC–coreceptor}$ (which is proportional to affinity of the MHC–coreceptor interaction) as obtained from the first set of simulations (scheme 1 in Fig. 1). At $k_{off} \sim 20\ s^{-1}$ the half-life is enhanced by ~1.2 times in the presence of coreceptor, whereas at $k_{off} \sim 80\ s^{-1}$ half-lives with and without coreceptor are statistically indistinguishable.

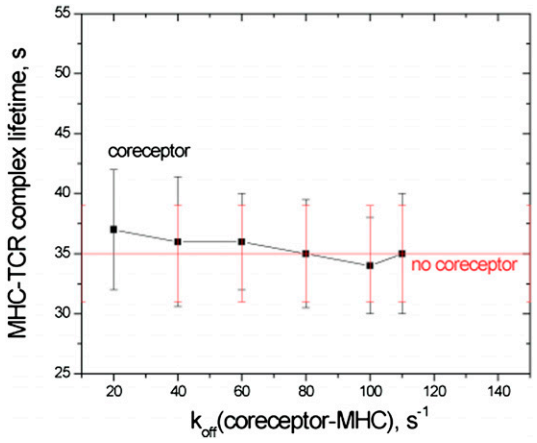

Fig. S2. Effective half-life of MHC on the T-cell surface as a function of $k_{off}^{MHC\text{-}coreceptor}$ (which is proportional to affinity of the MHC–coreceptor interaction) as obtained in the first set of simulations (scheme 1 in Fig. 1) with association between Lck and TCR set to zero [k_{on}(Lck–TCR) = 0]. One sees that in the absence of cooperative binding (Fig. 2*A*) MHC is not stabilized on the surface.

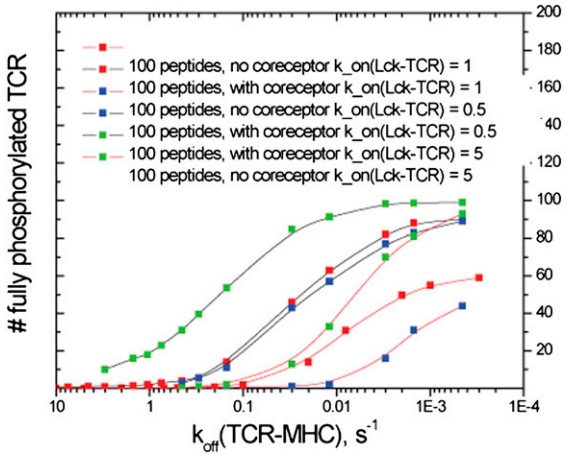

Fig. S3. Parameter sensitivity studies for k_{on}(Lck–TCR). Amount of fully phosphorylated TCR is plotted a function of peptide quality (as determined by $k_{off}^{TCR–pMHC}$). TCR phosphorylation with and without coreceptor is shown for three cases: k_{on}(Lck–TCR) = 0.5, 1, and 5 s^{-1} (the rest of the parameters are the same as in Table 1). Coreceptor-mediated enhancement does not change qualitatively when varying $k_{off}^{TCR–pMHC}$.

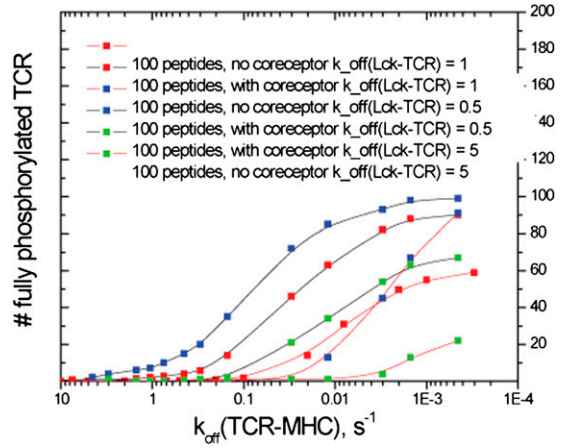

Fig. S4. Parameter sensitivity studies for k_{off}(Lck–TCR). Amount of fully phosphorylated TCR is plotted as a function of peptide quality (as determined by $k_{off}^{TCR–pMHC}$). TCR phosphorylation with and without coreceptor is shown for three cases: k_{off}(Lck–TCR) = 0.5, 1, and 5 s^{-1} (the rest of the parameters are the same as in Table 1). Coreceptor-mediated enhancement does not change qualitatively when varying $k_{off}^{TCR–pMHC}$.

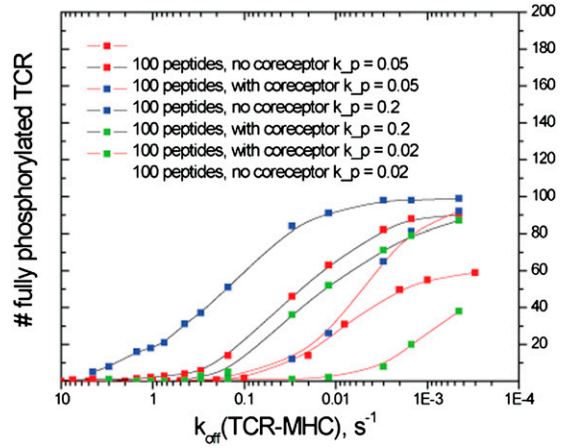

Fig. S5. Parameter sensitivity studies for k_p. Amount of fully phosphorylated TCR is plotted a function of peptide quality (as determined by $k_{off}^{TCR–pMHC}$). TCR phosphorylation with and without coreceptor is shown for three cases: k_p = 0.02, 0.05, and 0.2 s^{-1} (the rest of the parameters are the same as in Table 1). Coreceptor-mediated enhancement does not change qualitatively when varying k_p.

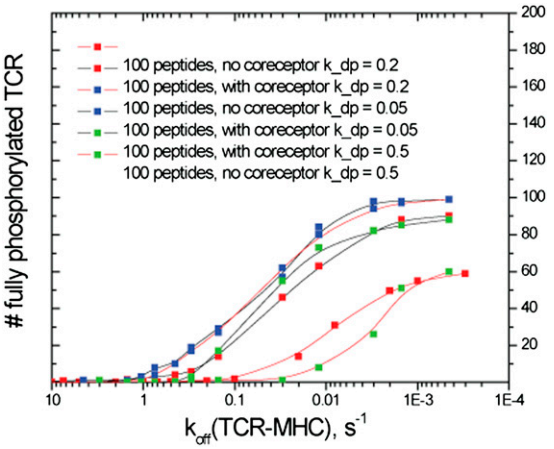

Fig. S6. Parameter sensitivity studies for k_{dp}. Amount of fully phosphorylated TCR is plotted as a function of peptide quality (as determined by $k_{off}^{TCR-pMHC}$). TCR phosphorylation with and without coreceptor is shown for three cases: k_{dp} = 0.05, 0.2, and 0.5 s^{-1} (the rest of the parameters are the same as in Table 1). Coreceptor-mediated enhancement does not change qualitatively when varying k_{dp}.

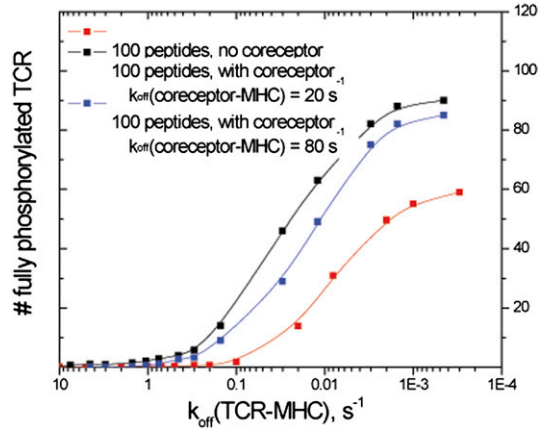

Fig. S7. Amount of fully phosphorylated TCR as a function of peptide quality (as determined by $k_{off}^{TCR-pMHC}$). Coreceptor-mediated enhancement does not change qualitatively when varying stability of coreceptor–MHC interactions between 20 s^{-1} (black curve) and 80 s^{-1} (blue curve).

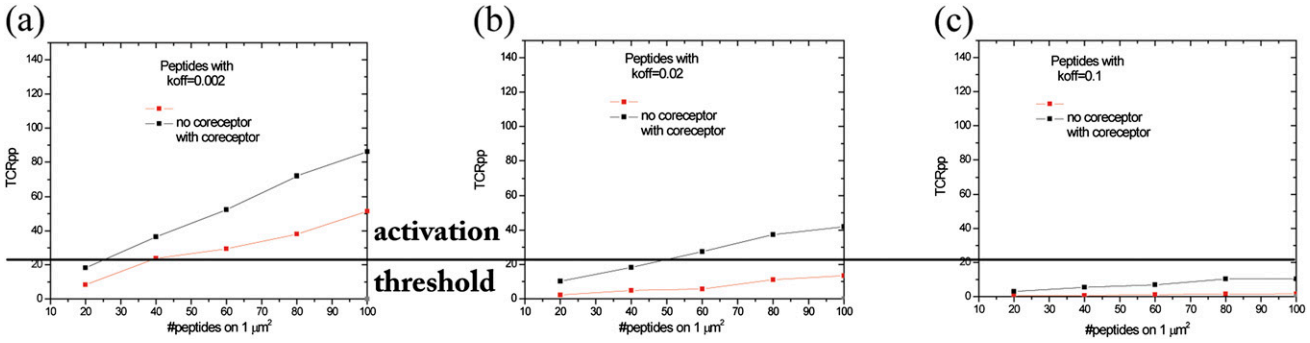

Fig. S8. Amount of fully phosphorylated TCR as a function of amount of peptides present in the contact area (dose–response curves) for strong agonist (*A*), typical agonist (*B*), and weak agonist (*C*).

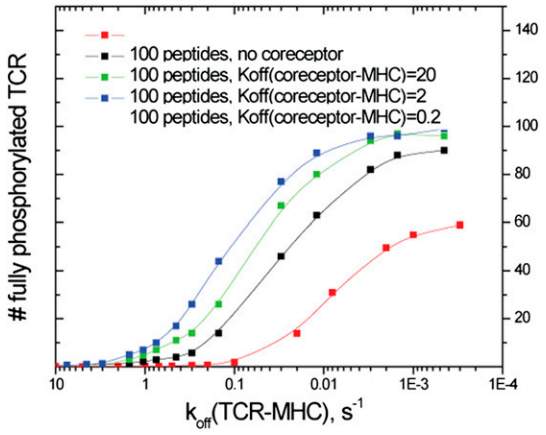

Fig. S9. Amount of fully phosphorylated TCR is plotted as a function of peptide quality (as determined by $k_{off}^{TCR-pMHC}$) for different interaction affinities between coreceptor and MHC (black, $k_{off}^{coreceptor-pMHC} = 20\ s^{-1}$; green, $k_{off}^{coreceptor-pMHC} = 2\ s^{-1}$; blue, $k_{off}^{coreceptor-pMHC} = 0.2\ s^{-1}$). The blue curve corresponds to the situation when affinity between coreceptor–MHC is similar to the affinity of cognate MHC-TCR interactions.

Other Supporting Information Files

Appendix S1 (DOC)